Published in final edited form as:
Anal Chem. 2010 February 1; 82(3): 967–973. doi:10.1021/ac902218y.

Integrated Microfluidic Device for Automated Single Cell Analysis using Electrophoretic Separation and Electrospray Ionization Mass Spectrometry

J. Scott Mellors[†], **Kaveh Jorabchi**[‡], **Lloyd M. Smith**[‡], and **J. Michael Ramsey**[†]

[†] Department of Chemistry, Chapman Hall Room 251, University of North Carolina at Chapel Hill, Chapel Hill, North Carolina 27599-3216

[‡] Department of Chemistry, 1101 University Avenue, University of Wisconsin-Madison, Madison, Wisconsin 53706

Abstract

A microfabricated fluidic device was developed for the automated real-time analysis of individual cells using capillary electrophoresis (CE) and electrospray ionization-mass spectrometry (ESI-MS). The microfluidic structure incorporates a means for rapid lysis of single cells within a free solution electrophoresis channel where cellular constituents were separated and an integrated electrospray emitter for ionization of separated components. The eluent was characterized using mass spectrometry. Human erythrocytes were used as a model system for this study. In this monolithically integrated device, cell lysis occurs at a channel intersection using a combination of rapid buffer exchange and an increase in electric field strength. An electroosmotic pump is incorporated at the end of the electrophoretic separation channel to direct eluent to the integrated electrospray emitter. The dissociated heme group and the α and β subunits of hemoglobin from individual erythrocytes were detected as cells continuously flowed through the device. The average analysis throughput was approximately 12 cells per minute demonstrating the potential of this method for high-throughput single cell analysis.

Introduction

The ability to perform chemical analysis on individual cells, termed chemical cytometry, is essential for measuring cell to cell variability and identifying differences between cells within a larger population.[1–6] Highly sensitive methods are required to detect and characterize the components of individual cells and the technology currently available is in most cases inadequate. [5] Single cell proteomics is perhaps the most challenging form of chemical cytometry due to the inherent difficulties associated with proteomics in general (difficulty in separating and identifying whole proteins, large number and great diversity of proteins present in most cells, large dynamic range of protein abundance, etc…).[7, 8]

Capillary electrophoresis (CE) has been the most commonly used separation method for chemical cytometry due to its high separation efficiency and small band volumes when using small diameter capillaries.[2, 9–14] The most commonly used detection method for single cell analysis has been laser induced fluorescence (LIF) due to its unmatched sensitivity and the ability to perform near-zero dead volume detection directly through fused silica CE capillaries.[1, 2, 10, 11, 15–20] Although cellular components are commonly derivatized with fluorescent

Supporting Information Available: This material is available free of charge via the internet at http://pubs.acs.org

tags, the native fluorescence of some proteins allows detection without labeling.[15, 17] Unfortunately, LIF detection provides little chemical information necessary for identification of the analytes. Mass spectrometry (MS) has been previously applied to single cell analyses to address this issue.[2, 21–23]

Two research groups have reported on the separation and detection of hemoglobin from individual erythrocytes using CE coupled to electrospray ionization-mass spectrometry (ESI-MS).[21, 22] In both cases, red blood cells were manually loaded into a prepared capillary while the researcher monitored the operation under a microscope. This tedious process is not practical for the analysis of large numbers of individual cells necessary to obtain statistically significant data regarding variability within a large population. A method for performing continuous lysis of erythrocytes using CE separation and LIF detection was described by Chen and Lillard. [15] The cells were introduced through one capillary and lysed at a junction to the inlet of a second CE capillary. The work presented here also uses a continuous cell delivery and lysis approach but all operations (i.e., cell delivery, lysis, separation of the lysate, and ionization for detection by MS of lysate components) are integrated on a single monolithic microfluidic device. Unlike the method performed by Chen and Lillard, this method does not require the use of a detergent for cell lysis and it utilizes a cell buffer that is compatible with CE-ESI-MS. This is the first report of continuous lysis of individual cells integrated with separation and MS detection of proteins from single cell lysate.

EXPERIMENTAL

Reagents and Materials

HPLC grade methanol, toluene, glacial acetic acid, and ammonium acetate were obtained from Fisher Chemical (Fairlawn, NJ). Sucrose was obtained from Mallinckrodt Baker, Inc. (Paris, KY). Purified deionized water was obtained from a Barnstead Nanopure Diamond water purifier fitted with a 0.2-μm filter (Barnstead International, Dubuque, IA). PolyE-323 was synthesized from 1, 2-bis(3-aminopropylamino)ethane and epichlorohydrin, both obtained from Sigma Chemical Company (St. Louis, MO), using a previously published procedure.[24] Trichloro(1H,1H,2H,2H-perfluorooctyl)silane was obtained from Sigma-Aldrich, Inc. (St. Louis, MO) and Oregon Green dye was procured from Molecular Probes (Eugene, OR).

Microchip Design

The microchip design used for this work combines two previously published microfluidic functional elements for individual cell lysis and CE-ESI.[25, 26] Figure 1 shows a schematic diagram of the device. The separation channel length measured from the cell lysis intersection to the electrospray corner was 4.7 cm. The isotropically etched channels had a full width of 75 μm and a depth of 10 μm. Unlike the previously published CE-ESI design this microchip incorporated a nano-channel segment (nanojunction) connecting the end of the separation channel to the electroosmotic (EO)-pump side channel. The nanojunction was approximately 100-nm deep and 200-μm long. It was incorporated to reduce the electroosmotic flow (EOF) in the side channel as a result of electric double layer (EDL) overlap to produce an EO pump.[27, 28] As described below, it was determined that a positively charged surface coating in the separation channel also produced an efficient EO pump.

Device Fabrication and Surface Modifications

Aside from the incorporation of the nanojunction, the microfluidic device used here was identical to the short channel CE-MS device described in our previous publication.[26] A more detailed description of the fabrication and surface coating procedures can be found there. Briefly, the microchip was fabricated from 150-μm thick Corning 0211 borosilicate glass substrates (Erie Scientific Co., Portsmouth, NH) using standard photolithography and wet

chemical etching. Unlike the previously described device, the photomask design incorporated a gap between the EO-pump side channel and the separation channel. After the channels were etched to a depth of approximately 10 μm the photoresist and chrome covering the gap were removed and a brief secondary etch to a depth of ~100 nm was performed to produce the nanojunction. All channel dimensions were measured with a KLA Tencor P15 surface profiler (KLA Tencor Corp., San Jose, CA).

All of the channels, except the EO-pump side channel, were coated with polyamine (PolyE-323), as was the case for the microfluidic CE-MS device.[26] The coating procedure was similar to other previously published protocols.[24, 29, 30] Briefly, a 15% (w/w) solution of PolyE-323, loaded into the reservoirs labeled B and C in figure 1, was pulled through the microfluidic channels for 1 hour by a vacuum applied at the electrospray corner. Excess polymer was then removed by flushing the channels with 50 mM ammonium acetate. The EO-pump side channel was filled with nanopure water during the coating procedure. The nanojunction greatly increased the hydrodynamic flow resistance of the side channel but did not affect the coating procedure since the side channel was not coated with polyamine.

The external surface of the electrospray corner was coated with perfluorooctylsilane to increase the hydrophobicity of the glass. This coating prevented fluid from accumulating at the channel exit and wetting the glass prior to the onset of electrospray. To coat the surface the corner was exposed to a mixture of 10% (v/v) trichloro(perfluorooctyl)silane in toluene for approximately 5 minutes. The surface was then rinsed with nanopure water and methanol to remove any unreacted silane. During the external surface coating procedure the microfluidic channels were filled with water to prevent the perfluorooctylsilane mixture from entering the channels as a result of capillary action. The surface coating was stable and did not produce any observable background ions in the mass spectra.

Electroosmotic Pump

The basic operation of the EO pump incorporated in the device has been previously described in detail.[26] Briefly, the microfluidic components of the pump consist of a tee intersection where the separation channel, the EO-pump side channel, and a short transport channel leading to the electrospray corner meet (figure 1). As mentioned above, all of the channels except the side channel were coated with a polyamine to reverse the surface charge on those channels. The EOF in both the separation channel and the side channel under normal operating conditions was in the direction towards the intersection near the electrospray corner. The EOF entering the tee intersection generates a pressure gradient that forces the fluid to exit at the electrospray tip.

The nanojunction connecting the separation channel to the EO-pump side channel was originally incorporated to create an EO pump in a device with uniform surface charge in all channels. The nanojunction diminished the EOF in the side channel by EDL overlap, generating a positive pressure on the separation channel side of the junction to allow effective convective transport of the CE eluent to the electrospray emitter. When using the cationic coating on the separation channel, the EOF in the separation and side channels were in opposite directions allowing creation of a positive pressure at the confluence, without the nanojunction. With the heterogeneous surface coatings in the two channels the nanojunction can be used to reduce the amount of dilution from the side channel buffer.

Chip Operation

The chip was operated by applying electric potentials to each of the four fluid reservoirs (figure 1) via platinum wire electrodes. The potentials were applied using a laboratory built power supply capable of independently controlling up to five different high voltage modules

(UltraVolt Inc., Ronkonkoma, NY), each with a maximum output of 10 kV. The power supply was connected to a personal computer via a SCB-68 breakout box that was in turn connected to a PCI-6713, 8-channel analog card (all from National Instruments, Austin, TX). A program written in LABVIEW (version 7.1) was used to control the power supply.

Figure 2 is a schematic diagram showing how the cell lysis CE-MS experiment was performed. The erythrocytes, suspended in cell buffer, were loaded into the cell reservoir, C. The buffer reservoirs, B, and the EO-pump side channel reservoir, SC, were filled with the CE-MS background electrolyte (a 50:50 mixture of methanol/water containing 2% acetic acid by volume). Voltages were applied to the reservoirs to maintain a steady flow of cells toward the lysis intersection, EOF from the lysis intersection to the end of the separation channel, and stable electrospray from the corner of the microchip. For the data presented here the voltages were as follows: 3.9 kV at the cell reservoir, 3.8 kV at each of the CE buffer reservoirs, and 8.8 kV at the EO-pump side channel reservoir. Due to the relatively high electrical resistance of the nanojunction and the difference in electrical conductivity between the cell buffer and the CE background electrolyte, most of the voltage drop occurred across the nanojunction. The voltage at the lysis intersection was estimated to be approximately 4 kV and the voltage at the electrospray corner approximately 5.5 kV. The voltage drop across the separation channel gave a separation field strength of approximately 300 V/cm. The field strength in the cell delivery channel was very low because of the relatively high electrical conductivity of the cell buffer. The flow in this channel may have been largely pressure-driven due to higher EOF in the channels filled with CE background electrolyte. The observed residence time for cells passing through this 8-mm long channel was approximately 30 seconds. The high electrospray voltage between the spray corner and the grounded MS inlet did not generate a corona discharge and produced a very fine spray plume. The electrode leads were insulated to prevent arcing. Safety procedures should always be followed when working with high voltage power supplies to minimize the risk of electric shock.

ESI-MS

The chip was mounted on an x-y-z translational stage in front of the atmospheric pressure inlet of a Micromass QTOF Micro mass spectrometer (Waters Corp., Milford, MA). The chip was positioned such that the spray corner was approximately 7 mm from the mass spectrometer inlet orifice. The electrospray plume was illuminated with a 3-mW green diode laser and imaged using a CCD camera mounted above the ionization source. Data were acquired using Masslynx version 4.0. The mass spectrometer was set to acquire over a mass to charge (m/z) range of 600–1000 at a rate of 0.24 s per summed scan with an interscan delay of 0.1 s. This m/z range was chosen to maximize the TOF pusher cycle speed and minimize background signal from the cell buffer.

Low Ionic Strength Cell Buffer

In order to prevent premature cell lysis it was necessary to keep the erythrocytes in an isoosmotic solution at neutral pH. Commonly used cell buffers such as phosphate buffered saline (PBS) could not be used because of their high electrical conductivity and incompatibility with ESI. Since flow within the microchip is controlled electrokinetically, large differences in conductivity between the cell buffer and CE background electrolyte made it difficult to optimize the flow rate and electrospray voltage. A low ionic strength solution (LISS)[31] containing ESI-compatible electrolytes was used to reduce the conductivity of the cell buffer relative to the CE-MS background electrolyte. The osmotic strength of the solution was increased to prevent cell lysis with the addition of a nonionic species. A variety of mixtures were tested, but the best results were obtained with a pH 7 solution of 260 mM sucrose and 15 mM ammonium acetate. The term LISS buffer used throughout this manuscript refers to this mixture. Visual inspection, via an optical microscope, of erythrocytes washed and suspended

in this buffer confirmed that the cells did not lyse and maintained their usual biconcave shape. The conductivity of the LISS buffer was measured to be 1.3 mS/cm. The conductivity of the CE-MS buffer (50:50 methanol/water containing 2% acetic acid) was measured to be 155 μS/cm. For comparison the conductivity of a normal PBS solution was measured to be 14.25 mS/cm. Conductivity measurements were made with a SevenMulti dual pH/conductivity meter (Mettler-Toledo GmbH, Schwerzenbach, Switzerland).

Preparation of Cell Suspension

A 5 μL aliquot of whole blood obtained from a healthy adult male was combined with 1 mL of sucrose/ammonium acetate LISS buffer. The cells were spun down in a centrifuge, washed twice with LISS buffer, and then diluted with LISS buffer to produce a concentration suitable for loading onto the microfluidic device (0.5 μL of blood per 1 mL of buffer). For the cell lysis CE-MS experiment, ~80 μL of the cell suspension was loaded onto the chip, corresponding to 40 nL of whole blood.

RESULTS AND DISCUSSION

The microchip was initially operated without any cells loaded onto the device, using LISS buffer in the cell reservoir to record the MS background from the buffer. Figure 3 shows a mass spectrum obtained by summing 1 minute of this data. The top trace shows the full mass range recorded (300–2000 m/z), while the bottom trace shows only the mass range recorded during the cell lysis experiment (600–1000 m/z). The y-axis of the bottom trace was also expanded to better show the less intense ions. The ions from the cell buffer were primarily protonated and sodiated clusters of sucrose, sucrose plus water, and fragmentation products from the breakage of sucrose glycosidic bonds. The strip function of MassLynx (v.4.0) was used to subtract the background mass spectrum shown in figure 3 from the data obtained during the cell lysis experiments.

Prior to the acquisition of MS data, the cell flow on the microchip was observed using fluorescence imaging to ensure that the cells were migrating to the lysis intersection and lysing properly. Approximately 1 mg of Oregon Green dye was added to a 1 mL suspension of red blood cells in LISS buffer and allowed to incubate for 50 minutes. The cells were pelleted, washed with LISS buffer, and then diluted to the same concentration used for the lysis-CE-MS experiments (0.5 μL of blood per 1 mL of buffer). Fluorescence imaging of the intersection region confirmed that the cells initially migrated slowly to the intersection, then rapidly accelerated and lysed as they entered the higher electric field after the intersection. Trace levels of Oregon Green dye in the cell buffer also allowed visualization of the buffer flow from the 3 channel segments leading into the intersection. Figure 4 is a screen capture from a CCD video taken of this process showing the dilution of the cell buffer as it flowed into the lysis intersection, along with 2 stained erythrocytes. The orientation of the video image matches the schematic diagram shown in figure 2, with the cells flowing from left to right through the lysis intersection. The erythrocyte on the right side of the intersection in figure 4 had already lysed. The full video is available via the internet as supplemental information. During this 29-s long video, 6 cells were observed flowing through the lysis intersection with apparently random spacing and no aggregation of cells. The 2 cells visible in figure 4 passed through the lysis intersection less than 1 second apart, approximately 8 seconds into the video clip. Although gradual settling of erythrocytes was observed in the cell reservoir, the rate of cells flowing through the device was relatively constant.

After proper flow and lysis of cells was verified using the fluorescence imaging microscope the chip was flushed with fresh buffer and mounted near the inlet of the mass spectrometer. Stable electrospray was established with cell-free LISS buffer in the cell reservoir and the background signal was recorded. The voltages were then turned off and the contents of the cell

reservoir replaced with the red blood cell suspension. Within a few minutes, after the voltages were reapplied, peaks corresponding to the dissociated heme group (616 m/z) and the α and β subunits of hemoglobin appeared in the MS signal. Data were acquired in 10 min increments. A representative total ion electropherogram is shown in figure 5. The top trace shows the raw data as it was recorded and the bottom trace shows the data after the strip function was used to subtract the background ions. All major peaks are coeluting α and β subunits of hemoglobin. A higher efficiency CE separation would enable resolution of these two components. As expected the peaks are randomly distributed over time and vary in intensity and width. Some of the variability in peak size may be due to differences in the hemoglobin content of individual erythrocytes; however it is likely that the larger peaks were caused by multiple cells passing though the lysis intersection at nearly the same time producing co-eluting peaks of heme or proteins.

Figure 6 shows the reconstructed selected ion electropherogram for the dissociated heme group (616 m/z) along with the background subtracted total ion count (TIC) over a 2 min time window. Upon lysis, each cell releases approximately 450 amoles of hemoglobin, which dissociates in the CE background electrolyte to yield 1.8 fmoles of protein subunit (2 α and 2 β from the hemoglobin tetramer) and one heme group for each subunit. The heme groups migrate through the separation channel faster than the protein subunits, so each cell lysis event generated a 616 m/z peak 10 s before a protein subunit peak (the large peaks visible in the TIC trace). The α and β subunits do not differ sufficiently in electrophoretic mobility to yield separate peaks in this relatively low efficiency CE separation, but the difference is great enough to cause the protein subunit peaks to be broader than the heme group peaks. Based on the fluorescence observations, it is believed that the majority of the peaks were the result of single cell lysis events. Under the fluorescence microscope it was clear that cells were not aggregating and individual cells could clearly be seen flowing through the device and lysing. Furthermore, the observed rate of cell lysis was approximately 0.2 cells per second, which agrees very well with the number of major peaks in the 616 m/z trace (approximately 23 peaks in 2 minutes). The peaks generated by the first 4 cell lysis events captured in the time window of figure 6 are labeled. The heme group peaks of cells 2 and 3 were only partially resolved (figure 6, top) due to the spatial/temporal proximity of the cells arrival at the lysis intersection, while the corresponding protein subunit peaks eluted as a single, wider peak (figure 6, bottom). The remaining peaks are not labeled, but the correlation between peaks in the two traces is easily discernable.

Figure 7 shows mass spectra generated from the three regions indicated by gray rectangles in the bottom trace of figure 6. The top spectrum (A) shows a baseline region where no cell lysis events occurred. Ions corresponding to hemoglobin (both protein and heme group) were detected in the baseline, indicating that either some cells had lysed prematurely, or hemoglobin had leaked out of some cells before lysis. The use of a different cell buffer might correct this problem. The middle spectrum (B) corresponds to a peak that is believed to be the protein subunits from a single erythrocyte. The α and β subunit ions are labeled in this spectrum. The charge states observed range from +16 to +22 for the β subunit and from +18 to +24 for the α subunit. The bottom spectrum (C) corresponds to one of the larger peaks observed in figure 6. This peak may have resulted from the lysis of a cell with greater than average hemoglobin content, but it may also be the result of the simultaneous lysis of multiple cells. Interestingly both subunit peak spectra (B and C) show a rise in the 616 m/z (heme group) signal above the baseline level. This may suggest that a small percentage of heme groups remain associated with the protein subunits throughout the electrophoretic separation and do not dissociate until ESI occurs. Further studies are required to explore this phenomenon.

We were able to operate the device for approximately 1 hr before the buildup of cellular debris near the lysis intersection degraded the performance. Observation under a light microscope

indicated that this build-up was initiated when a cell stuck to the channel wall near the lysis intersection. Later arriving cells had a tendency to stick to this cell, leading to a gradual build-up of material. There was no evidence of lysed cells adhering to the separation channel. Flushing of the device with a common detergent (Contrad 70, Decon Labs, Inc., King of Prussia, PA) removed the debris, and after recoating with polyE-323 performance of the device was restored. It has not yet been determined how many times the device can be cleaned and reused.

SUMMARY AND CONCLUSIONS

The fully integrated microfluidic device described here was capable of performing continuous on-chip lysis of erythrocytes with real-time electrophoretic separation and ESI of hemoglobin. The use of a LISS cell buffer enabled stable electrokinetic operation of the device. Although the cell buffer produced a relatively large MS background signal, this background could be subtracted from the cell lysis data allowing the protein and heme group peaks to be easily detected and identified. The sensitivity of our mass spectrometer precluded the detection of the next most abundant protein in erythrocytes, carbonic anhydrase I (~7 amol/cell).[32, 33]

Improvements in ESI-MS sensitivity and separative performance would obviously increase the value of the experiments described in this paper. It has been shown that ESI-MS sensitivity improves as the flow rate is decreased.[34, 35] The sensitivity of this device may be improved by optimizing the channel dimensions to produce the lowest possible flow rate while still allowing free flow of cells. The use of smaller channel dimensions would allow high separation field strength for optimal CE performance while also minimizing dilution of the cell contents to maximize ESI-MS sensitivity. Isotropic etching places a limit on the aspect ratio of the channels that can be produced, so it may be necessary to use an anisotropic method like deep reactive ion etching (DRIE)[36] to produce channels that are closer to the diameter of the cells in both width and height. Mass spectrometers with better sensitivity will also obviously improve detection limits. Improved separative performance and alternative separation mechanisms beyond CE are easily incorporated into devices such as we describe. Future work will explore options to maximize the sensitivity of this method and improve separative performance to expand its utility.

Erythrocytes are uniquely suited to the single cell analysis method described here. They freely flow through microfluidic channels and lyse easily, they have a high concentration of an easily detected protein, and they have a relatively simple cellular structure. Other types of cells would likely pose a greater challenge to this type of analysis. The work of McClain and coworkers demonstrated a microfluidic device for single cell analysis of more complex nonadherent cells.[25] In that work Jurkat cells loaded with fluorogenic dyes were electrically lysed on chip. Hydrodynamic flow was used to direct the cellular debris to waste while the dyes were electrokinetically transported into an orthogonal channel for electrophoretic separation and LIF detection. Such a strategy could be coupled with the ESI-MS interface described here to address cytosolic proteins and potentially proteins contained within organelles with appropriate lysis measures. The speed and sensitivity of the mass spectrometer and the efficiency of the separation must be improved to enable rapid detection of less abundant cellular components.

Supplementary Material

Refer to Web version on PubMed Central for supplementary material.

Acknowledgments

This research was sponsored by the National Heart Lung and Blood Institute proteomics initiative under Grant N01-HV-28182. The authors thank Waters Corp. for providing the Qtof micro mass spectrometer.

References

1. Krylov SN, Arriaga E, Zheru Z, Chan N, Palcic MM, Dovichi NJ. Cytometry 1999;37:14–20. [PubMed: 10451502]
2. Swanek, FD.; Ferris, SS.; Ewing, AG. Handbook of Capillary Electrophoresis. 2. Landers, JP., editor. CRC Press; Boca Raton, FL: 1997. p. 495-544.
3. Turner EH, Cohen D, Pugsley HR, Gomez DG, Whitmore CD, Zhu C, Dovichi NJ. Anal Bioanal Chem 2008;390:223–226. [PubMed: 17955216]
4. Price AK, Culbertson CT. Anal Chem A-Pages 2007;79:2614–2621.
5. Borland LM, Kottegoda S, Phillips KS, Allbritton NL. Annual Review of Analytical Chemistry 2008;1:191–227.
6. Dovichi NJ, Hu S. Current Opinion in Chemical Biology 2003;7:603–608. [PubMed: 14580565]
7. Domon B, Aebersold R. Science 2006;312:212. [PubMed: 16614208]
8. Ye M, Jiang X, Feng S, Tian R, Zou H. Trends in Anal Chem 2007;26:80–84.
9. Huang WH, Ai F, Wang ZL, Cheng JK. J Chromatogr B 2008;866:104–122.
10. Krylov SN, Dovichi NJ. Electrophoresis 2000;21:767–773. [PubMed: 10733220]
11. Krylov SN, Starke DA, Arriaga EA, Zhang ZR, Chan NWC, Palcic MM, Dovichi NJ. Anal Chem 2000;72:872–877. [PubMed: 10701276]
12. Li SFY. Capillary Electrophoresis; principles, practice and applications. Journal of Chromatography Library: Amsterdam, The Netherlands. 1996
13. Lukacs KD, Jorgenson JW. J High Res Chromatogr and Chromatogr Comm 1985;8:407–411.
14. Zabzdyr JL, Lillard SJ. Trac-Trend Anal Chem 2001;20:467–476.
15. Chen SJ, Lillard SJ. Anal Chem 2001;73:111–118. [PubMed: 11195493]
16. Cheng YF, Dovichi NJ. Science 1988;242:562–564. [PubMed: 3140381]
17. Hellmich W, Pelargus C, Leffhalm K, Ros A, Anselmetti D. Electrophoresis 2005;26:3689–3696. [PubMed: 16152668]
18. Johnson ME, Landers JP. Electrophoresis 2004;25:3513–3527. [PubMed: 15565706]
19. Krylov SN, Arriaga E, Zhang ZR, Chan NWC, Palcic MM, Dovichi NJ. J Chromatogr B 2000;741:31–35.
20. Lillard SJ, Han FT, Chen SJ, Zabzdyr JL, McCoy CE, Shaker R. Abstr Pap Am Chem Soc 2000;220:U102–U102.
21. Cao P, Moini M. J Am Soc Mass Spectr 1999;10:184–186.
22. Hofstadler SA, Severs JC, Smith RD, Swanek FD, Ewing AG. Rapid Commun Mass Spectrom 1996;10:919–922. [PubMed: 8777325]
23. Rubakhin SS, Churchill JD, Greenough WT, Sweedler JV. Anal Chem 2006;78:7267–7272. [PubMed: 17037931]
24. Hardenbourg E, Zuberovic A, Ullsten S, Soderberg L, Heldin E, Markides KE. J Chromatogr A 2003;1003:217–221. [PubMed: 12899312]
25. McClain MA, Culbertson CT, Jacobson SC, Allbritton NL, Sims CE, Ramsey JM. Anal Chem 2003;75:5646–5655. [PubMed: 14588001]
26. Mellors JS, Gorbounov V, Ramsey RS, Ramsey JM. Anal Chem 2008;80:6881–6887. [PubMed: 18698800]
27. Burgeen D, Nakache FR. J Phys Chem 1964;68:1084–1091.
28. Hu JS, Chao CYH. Sensor Actuat a-Phys 2007;135:273–282.
29. Akashi S, Suzuki K, Arai A, Yamada N, Suzuki E, Hirayama K, Nakamura S, Nishimura Y. Rapid Commun Mass Spectrom 2006;20:1932–1938. [PubMed: 16715472]
30. Ullsten S, Zuberovic A, Wetterhall M, Hardenbourg E, Markides KE, Bergquist J. Electrophoresis 2004;25:2090–2099. [PubMed: 15237410]
31. Harshman S, Najjar VA. Biochem Biophys Res Comm 1963;11:411.
32. Akbar SA, Brown PR. Clin Biochem 1996;29:157–164. [PubMed: 8601325]
33. Lindskog S. Pharmacol Therapeut 1997;74:1–20.

34. Valaskovic GA, Kelleher NL, Little DP, Aaserud DJ, Mclafferty FW. Anal Chem 1995;67:3802–3805. [PubMed: 8644926]
35. Wilm M, Mann M. Anal Chem 1996;68:1–8. [PubMed: 8779426]
36. Thienot E, Domingo F, Cambril E, Gosse C. Microelectron Eng 2006;83:1155–1158.

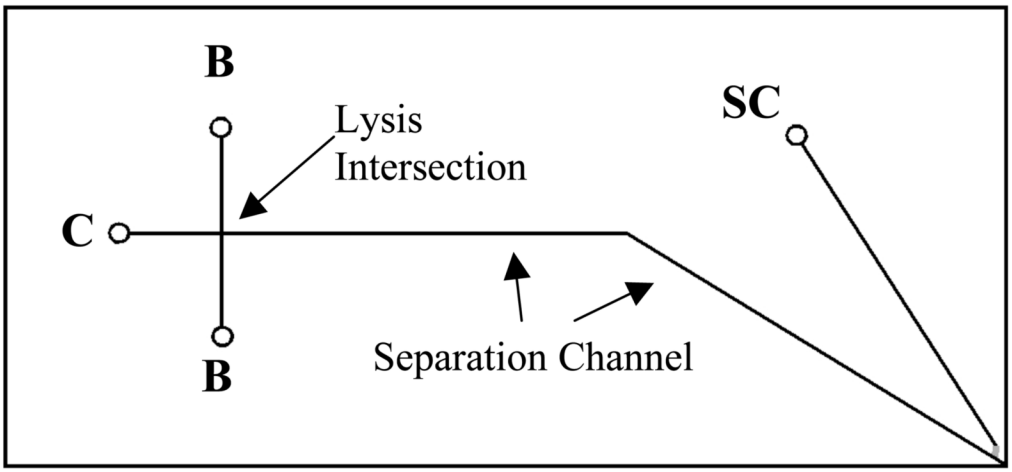

Figure 1.
Schematic diagram showing the design of the cell lysis CE-MS microchip. Reservoirs are labeled C (cells), B (buffer), and SC (EO-pump side channel). The separation channel is 4.7-cm long, measured from the cell lysis intersection to the electrospray corner. A nanojunction (~100-nm deep) connects the EO pump side channel to the separation channel.

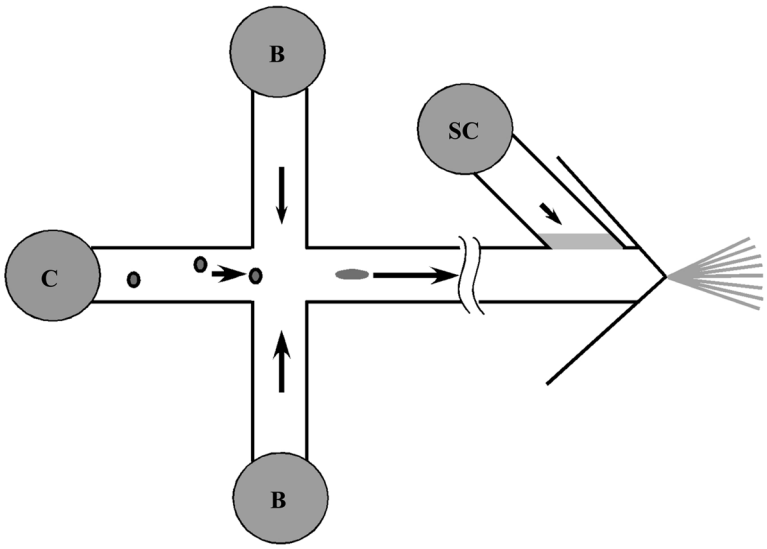

Figure 2.

Schematic diagram showing the basic operation of the cell lysis CE-MS microchip. Reservoirs are labeled as described in figure 1. The arrows indicate the direction and relative magnitude of electroosmotic flow. The cells migrate toward the lysis intersection, at which point the increased electric field and the rapid dilution of the cell buffer causes the cells to quickly lyse. An electrophoretic separation then occurs as the cell contents migrate toward the electrospray orifice where electrospray ionization occurs.

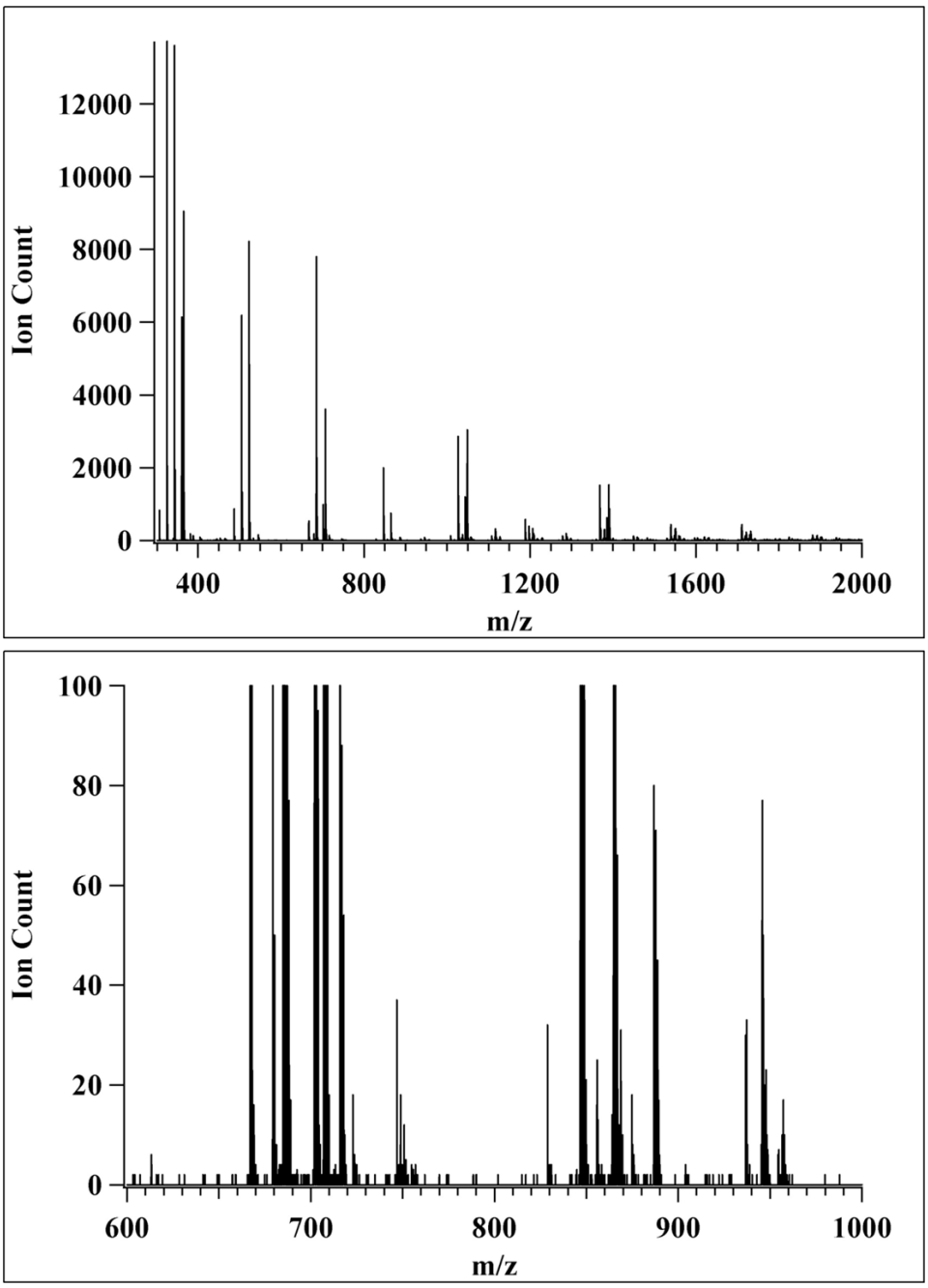

Figure 3.

1 minute summation of the background MS signal acquired with no cells present in the cell buffer. The major peaks correspond to protonated and sodiated sucrose clusters. The top trace shows the full m/z range measured (300–2000), and the bottom trace shows the m/z range used for the cell lysis experiment (600–1000). In the bottom trace the y-axis range was expanded to better show the less intense ions.

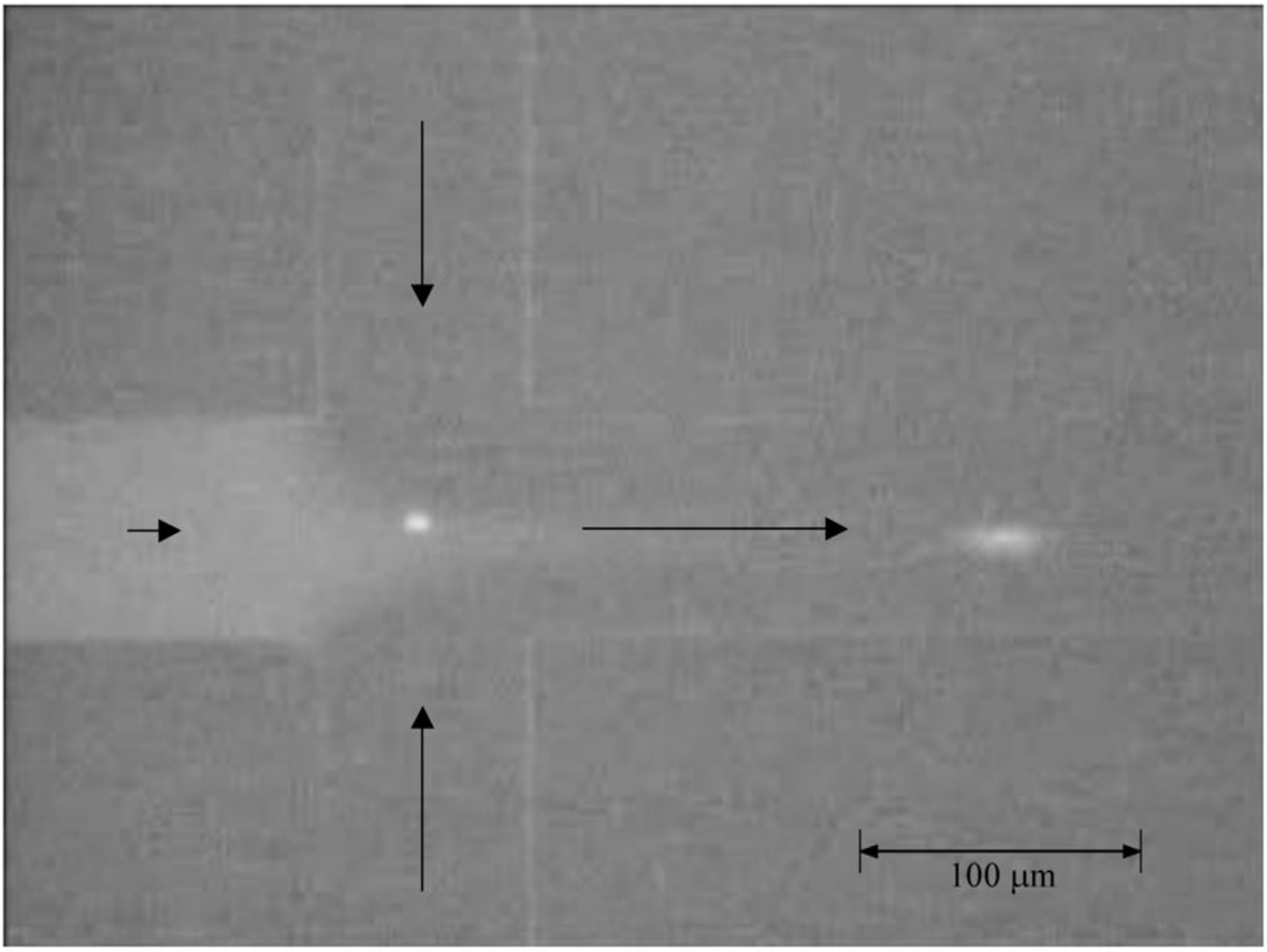

Figure 4.
Frame capture from a CCD video taken on a fluorescence microscope showing Oregon Green stained erythrocytes moving (from left to right) from the cell reservoir through the lysis intersection and into the separation channel. The cell on the right of the injection intersection has already lysed. The cell buffer contained Oregon Green dye that was not fully washed from the cell suspension, so the flow out of the different channels can be seen. The arrows indicate the direction of EOF in the channels.

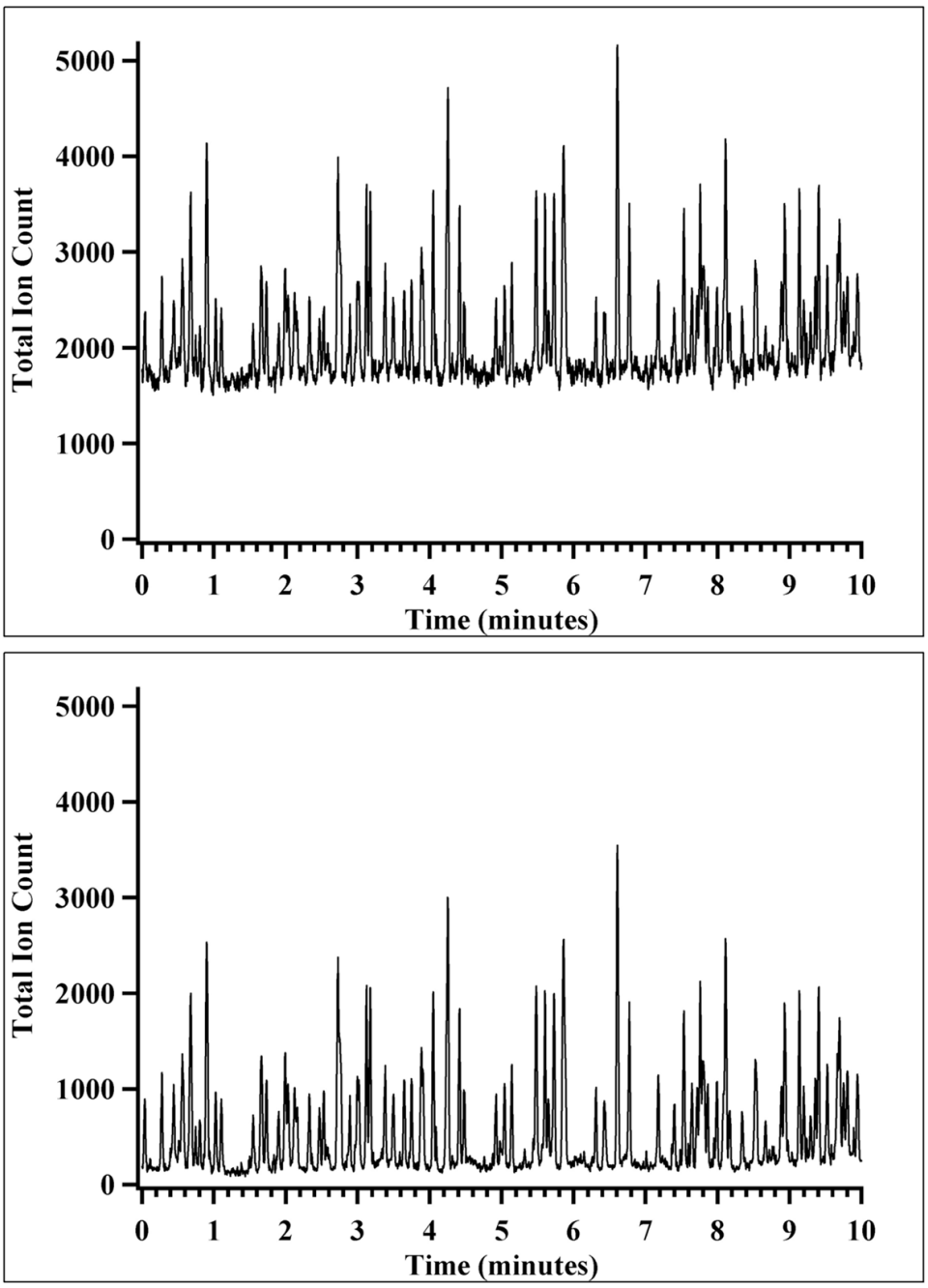

Figure 5.
Raw (top) and background subtracted (bottom) total ion count measured over 10 minutes of continuous erythrocyte lysis/CE-MS. The peaks correspond to the α and β subunits of hemoglobin.

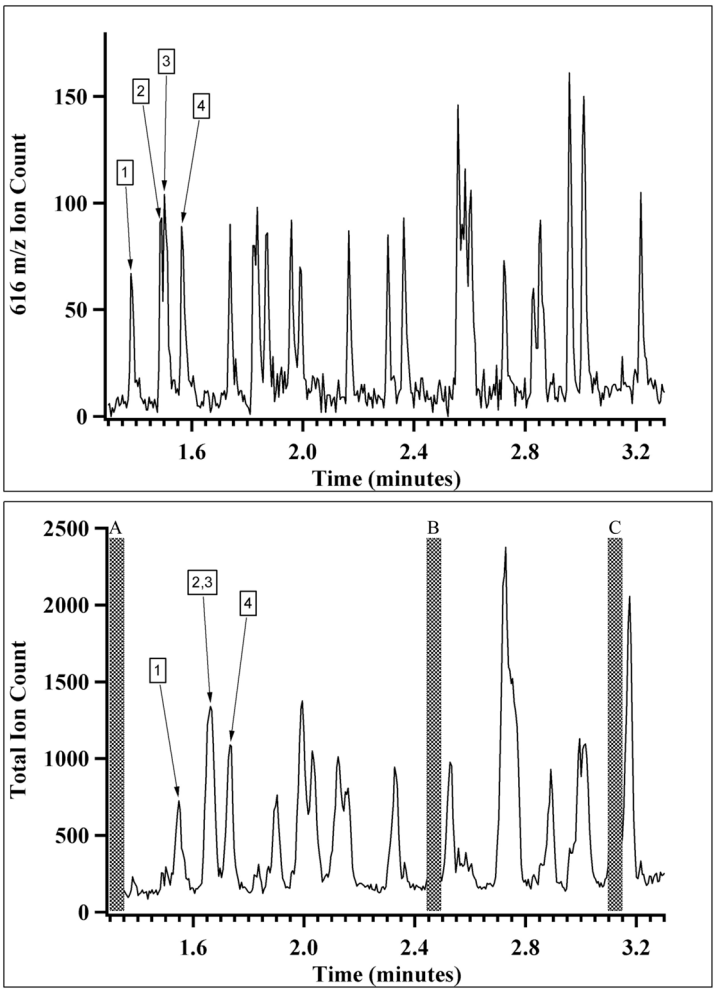

Figure 6.

The ion count at 616 m/z corresponding to the dissociated heme groups (top) and the background subtracted total ion count (bottom) for a 2 minute segment of the continuous lysis/CE-MS experiment. The dissociated heme groups migrated faster through the separation channel, so each lysis event generated a 616 m/z peak approximately 10 seconds before the major peak (visible in the TIC) corresponding to the α and β hemoglobin subunits. The peaks corresponding to the first 4 cell lysis events observed in this detection window are labeled in both traces to help illustrate the trend which continues throughout the entire run. The gray rectangles correspond to the data that was used to generate the spectra labeled with the same letters in figure 7.

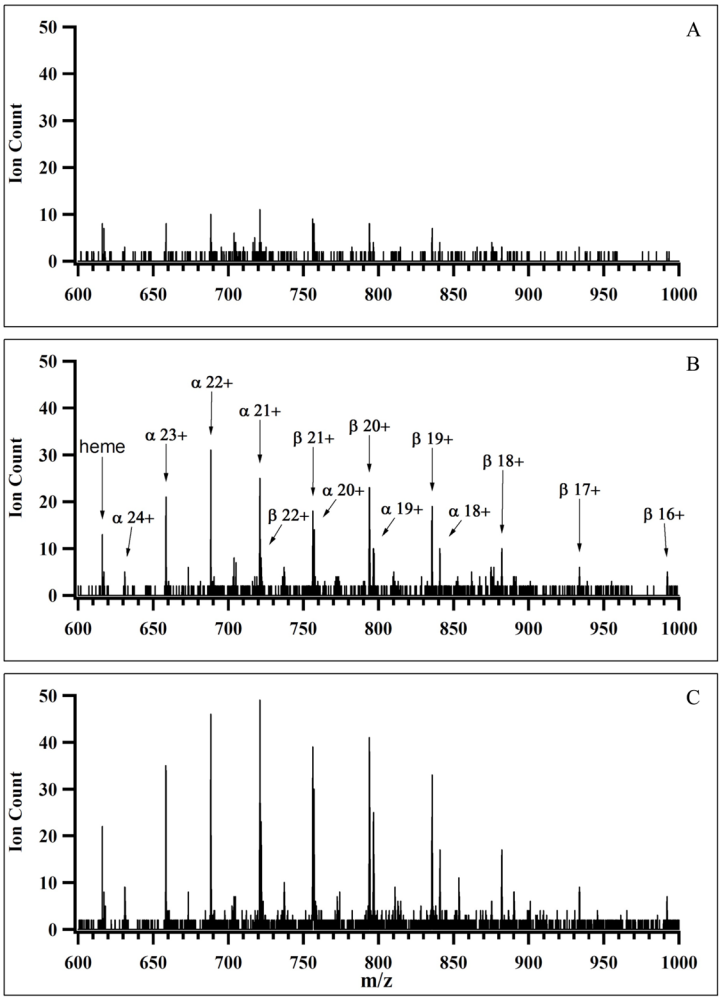

Figure 7.

Mass spectra generated by summing the data in each of the 3 second wide windows illustrated by gray rectangles in figure 6. The top trace (A), corresponds to the baseline, the middle trace (B) corresponds to a single cell lysis event, and the bottom trace (C) either corresponds to the lysis of a cell with greater than average hemoglobin content, or the simultaneous lysis of multiple cells.